Original Article

Establishment of a normal control model of children's brain 18-fluorodeoxyglucose positron emission tomography and analysis of the changing pattern in patients aged 0–14 years

Yao Wang[1]^, Jiajie Mo[2], Yu Sun[1], Hao Yu[1], Chang Liu[1], Qingzhu Liu[1], Yan Fan[3], Shuang Wang[4], Xiaoyan Liu[4], Yuwu Jiang[1,4], Lixin Cai[1]

[1]Pediatric Epilepsy Center, Peking University First Hospital, Beijing, China; [2]Department of Neurosurgery, Beijing Tiantan Hospital, Capital Medical University, Beijing, China; [3]Department of Nuclear Medicine, Peking University First Hospital, Beijing, China; [4]Department of Pediatrics, Peking University First Hospital, Beijing, China

Contributions: (I) Conception and design: Y Wang, J Mo, L Cai; (II) Administrative support: Y Jiang, X Liu; (III) Provision of study materials or patients: H Yu, C Liu, Q Liu; (IV) Collection and assembly of data: Y Wang, Y Sun; (V) Data analysis and interpretation: H Yu, Y Fan, S Wang; (VI) Manuscript writing: All authors; (VII) Final approval of manuscript: All authors.

Correspondence to: Lixin Cai, MD. Pediatric Epilepsy Center, Peking University First Hospital, No. 1 Xi'anmen St., Xicheng District, Beijing 100032, China. Email: PUFHPEC_CLX@163.com.

Background: It is difficult to obtain 18-fluorodeoxyglucose positron emission tomography (^{18}FDG-PET) data from normal children, and changes in brain metabolism in children due to growth and development are poorly understood. For the first time, we established a normal control model of brain ^{18}FDG-PET in children and evaluated its feasibility. The association of PET with age in children aged 0–14 years was analyzed. This study aimed to establish a normal control model of brain ^{18}FDG-PET in children for the first time and to verify its feasibility, and to analyze the trend of PET with age in children aged 0–14 years.

Methods: In this retrospective cohort study, the ^{18}FDG-PET imaging data of patients with no epileptiform discharge involvement contralateral to the epileptogenic zone were consecutively collected from January 2015 to June 2022 according to strictly defined screening criteria. For the normal control data, the hemisphere contralateral to the epileptogenic zone was mirrored and spliced to form an intact brain. The cohort of children aged 0–14 years was divided into 14 groups according age by year. Subsequently, patients who underwent lesionectomy with clear hypometabolism that roughly coincided with the extent of surgical resection were examined. The PET scan was compared with the control model, and the ratio of overlapping parts (hypometabolic areas ∩ surgical resection area) to hypometabolic parts (ROH) was calculated. Multiple regression analysis was performed on the normal control model for every 3- to 4-year age interval.

Results: A total of 159 normal control models were established. Five patients were randomly selected to verify the reliability of each yearly model. The average ROH was 0.968. Metabolism increasing with age in the different brain regions was observed at ages 0–2~, 3–5~, and 6–10 years. No age-related metabolic increase or decrease was found in the 10- to 14-year-old group. The metabolism in the 7- to 8-year-old group was higher than that in the 13- to 14-year-old group.

Conclusions: With strict screening criteria, the method of mirroring the contralateral hemisphere of the epileptic zone and splicing it into a complete brain as a means of creating a normal control group is feasible. The method offers convenience to the studies that lack healthy pediatric controls. Children under 10 years of age (especially 0–6 years old) experience considerable metabolic changes year on year. After the age of

^ ORCID: 0000-0003-1074-5375.

10 years, the changes in metabolism gradually decrease, and metabolism also slowly decreases. Our findings provide guidance the clinical interpretation of areas with hypometabolism and emphasize the importance of establishing a normal control model of the child's brain, which should not be replaced by an adult model.

Keywords: 18-fluorodeoxyglucose positron emission tomography (^{18}FDG-PET); children; normal control; changing pattern

Submitted Dec 20, 2023. Accepted for publication May 23, 2024. Published online Jun 27, 2024.
doi: 10.21037/qims-23-1809
View this article at: https://dx.doi.org/10.21037/qims-23-1809

Introduction

Neuroimaging has been used to analyze brain networks in multiple studies, as image analysis guarantees a relatively comprehensive spatial coverage of all networks (1-3). Network research based on magnetic resonance imaging (MRI) and positron emission tomography (PET) is particularly common (4-6). However, network analysis often requires intergroup comparisons with normal controls (3,5,7), and thus the availability of normal control data is particularly critical. Furthermore, normal control data can also be applied to lesion detection, prediction of pre and postoperative surgical success, planning of the stereoelectroencephalography (SEEG) approach, postoperative identification of residual lesion, etc.

Among adults or older children, there are often patients who undergo brain PET due to other diseases outside the nervous system. These data can often be used as normal control data and are relatively easy to obtain (3,8). In children, the most common extracranial disease is tumors. The treatment of oncology may bring potential downsides to intracranial PET results even if there are no obvious intracranial lesions. Moreover, obtaining data on PET in younger children (i.e., 0–2 years of age) is a nearly universal challenge (9,10). Due to factors such as growth and development in children, the PET of adults is not universally applicable, which poses considerable obstacles to pediatric brain network PET analysis. Therefore, this study was designed to develop a method for establishing normal control data, with the aim of compensating for the lack of a normal control group in pediatric PET.

There is no consensus regarding the relationship between changes in cranial PET metabolism and age in children. Chugani *et al.* concluded that brain metabolism reaches its peak between the ages of 8 and 10 years (11). A study from Cruz-Cortes *et al.* showed that brain glycolytic metabolism increased with age until 13 years old (9). An established PET model can not only be used to analyze brain networks but also simulate brain metabolism in different age groups. Based on this, the changes in brain PET during normal children's growth and development can be clarified, providing a theoretical basis for future research. We present this article in accordance with the STROBE reporting checklist (available at https://qims.amegroups.com/article/view/10.21037/qims-23-1809/rc).

Methods

Establishment of the PET normal control model

In this retrospective cohort study, the preoperative 18-fluorodeoxyglucose positron emission tomography (^{18}FDG-PET) data of patients with epilepsy aged 0–14 years who underwent resective surgery in Pediatric Epilepsy Center, Peking University First Hospital, from January 2015 to June 2022 were consecutively collected. The PET scanning time was within 6 months before surgery. All patients were seizure free after at least 1 year of follow-up and met the following conditions : (I) focal seizure, without epileptic spasms or other types of generalized seizure; (II) focal interictal and ictal electroencephalograms (EEGs), with no interictal discharges in the hemisphere contralateral to the lesion; (III) lesionectomy without multilobe and hemispheric surgery; (IV) development quotient (DQ; Griffiths Development Scales-Chinese Edition <6 years old) or intelligence quotient (IQ; Wechsler Intelligence Scale ≥6 years old) >70 (12,13); and (V) whole-exome sequencing indicating no abnormal gene variation. The selection of patients was discussed and decided by neurosurgeons, physicians, and neuroelectrophysiologists specializing in epilepsy.

This study was conducted in accordance with the Declaration of Helsinki (as revised in 2013) and was approved by the Institutional Review Board of Peking University First Hospital (protocol code: 2022-306-001;

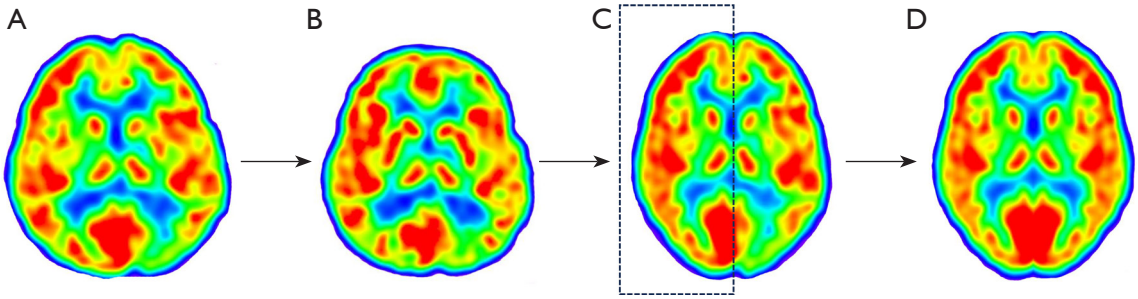

Figure 1 Modeling process for the normal control group. (A) PET scan in a 6-year-old female patient meeting the inclusion criteria and with FCD in the left occipital lobe. The PET scan was normalized onto pediatric templates (4.5- to 8.5-year-old atlas) (B). The PET scan was then normalized onto MNI 152 templates. The right hemisphere (dashed box) was selected and mirrored (C). A complete brain was spliced with the right hemisphere and mirrored hemisphere (D). FCD, focal cortical dysplasia; PET, positron emission tomography; MNI, Montreal Neurological Institute.

date: July 7, 2022). Informed consent was obtained from patients' parents or legal guardians.

^{18}FDG-PET data acquisition

The PET examinations were performed under standard resting conditions using the Gemini GXL PET-CT system (Philips, Amsterdam, the Netherlands) under the following parameters: field of view (FOV) =300 mm, matrix 128×128, and slice thickness 2 mm. The ^{18}FDG was injected intravenously at a mean dose of 3.7 MBq/kg body weight. Prior to the PET examination, most younger children under 3 years old were sedated orally with chloral hydrate. The nil per os time was 6 hours. The uptake time was 60 minutes, and the acquisition time for the scans was 10 minutes. The children were placed in a dark, quiet room during uptake.

Methods for establishing the model

Model building was performed using MATLAB software (MathWorks. Inc., Natick, MA, USA) and the voxel-level using SPM12 software (Wellcome Department of Cognitive Neurology, University College London, London, UK; http://www.fil.ion.ucl.ac.uk/spm/software/spm12/). The PET images that met the above-mentioned requirements were spatially normalized onto the Montreal Neurological Institute (MNI) pediatric template (14,15) based on age and then spatially normalized onto the MNI 152 template (voxel size: 1 mm × 1 mm × 1 mm) (https://nist.mni.mcgill.ca/atlases/). For the normal control data, the hemisphere contralateral to the epileptogenic zone was mirrored and spliced with it to form an intact brain. According to the age at which PET examination was performed, the collection of models was divided into 14 groups with each group being 1 year (i.e., 0~, 1~, ... 13~) (*Figure 1*).

Reliability validation of the model

Patient selection

(I) Patients underwent resection confined to one lobe and were seizure free for at least 1 year of postoperative follow-up. Most patients continued on antiepileptic drugs 1 year after surgery. The majority of patients ceased taking antiepileptic drugs around 2 years after surgery. (II) PET hypometabolism was evident by visual observation (at least one epilepsy surgeon and a nuclear medicine physician) and was confined to the area of surgical resection. Five patients per age group were randomly selected for validation (16).

Methods for validation

With the same grouping described above, the set of PET scans for validation was also divided into 14 groups according to age. Preoperative MRI for validation was aligned and normalized to the MNI space. With reference to the extent of surgical resection shown by postoperative thin-scan CT or 3D T1-weighted MRI, the volumes of interest (VOI) of the surgical resection area (Vm) were extracted from preoperative MRI. Normal control PET scans were smoothed with a Gaussian filter [8-mm full width half maximum (FWHM)]. The PET scan for validation was aligned, smoothed, and normalized by the same method described above. Subsequently, the PET scan was standardized to reduce individual variation (17). The images of the verified PET scan were each compared with those of a group of age-matched control PET scans using

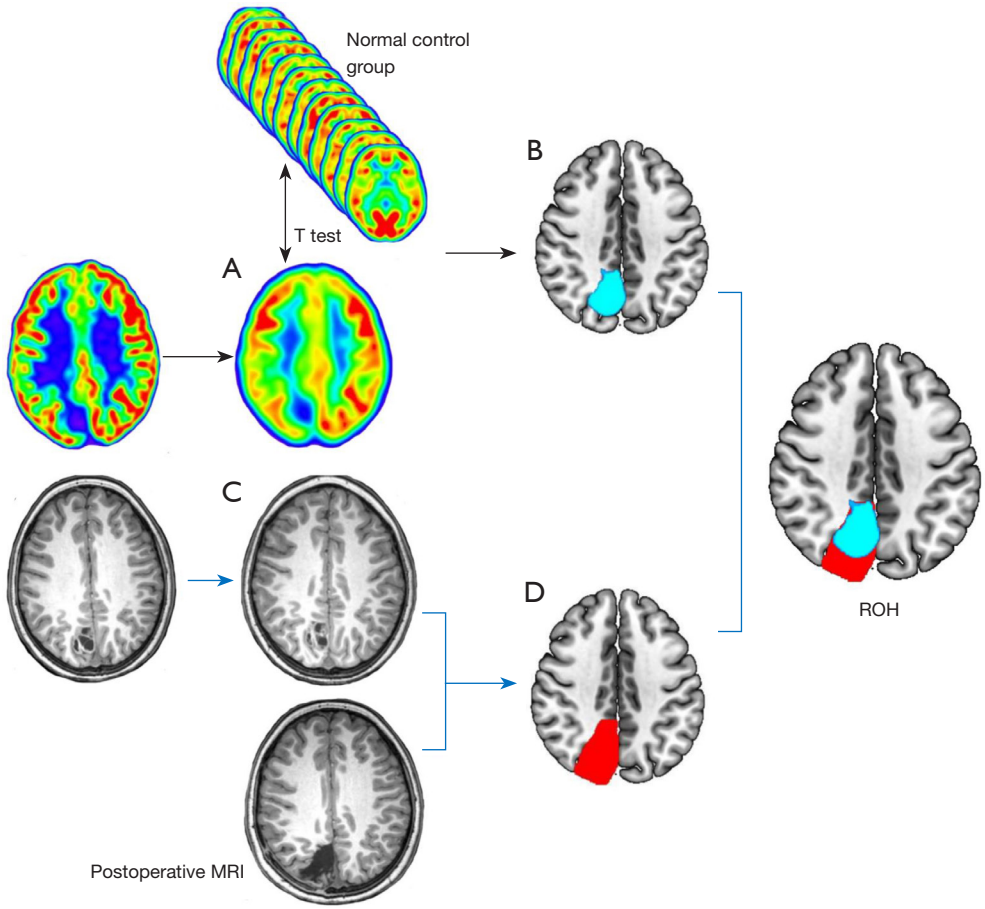

Figure 2 The process of model validation. The patient was an 8-year-old boy and met the inclusion criteria. LEAT with localized hypometabolism was present in the right parietal lobe. The PET scan was normalized onto pediatric templates and then onto MNI 152 templates. (A) The PET scan after smoothing and standardization. (B) Compared with the 8~-year-old normal control data, the largest brain regions with differences in metabolism were selected and saved as the VOI. (C) Preoperative MRI of the patient was aligned and normalized to the MNI space by the method described above. (D) Based on the postoperative MRI, the VOI of the surgical resection area was extracted. ROH was calculated from the ratio of VOIs of (B) and (D). LEAT, long-term epilepsy-associated tumor; PET, positron emission tomography; MNI, Montreal Neurological Institute; VOI, volume of interest; MRI, magnetic resonance imaging; ROH, ratio of overlapping parts to hypometabolic parts.

voxel-based independent *t*-test analysis. The statistical parametric mapping (SPM) maps included a threshold of $P<0.001$ (two-sided) corrected for multiple comparisons with the false-discovery rate (FDR) method. A cluster threshold of 50 voxels was applied. After comparison, the largest hypometabolic region (Vp) was selected, and the overlap between it and the surgically resected region (Vm) was calculated ($Vr = Vp \cap Vm$). Finally, the ratio of Vr to Vp was calculated [ratio of overlapping parts to hypometabolic parts (ROH)] (*Figure 2*).

The pattern of PET scan changes for ages 0–14 years

Whole-brain multiple regression analyses were performed on the following groups: 0–2~ (0~, 1~, 2~), 3–5~ (3~, 4~, 5~), 6–9~ (6~, 7~, 8~, 9~), and 10–13~ (10~, 11~, 12~, 13~). The threshold setting parameters were the same as those used previously, and the software used for the analysis was SPM12 (Wellcome Trust Centre for Neuroimaging, Institute of Neurology, University College London). This study was approved by the Institutional Review Board of Peking University First Hospital.

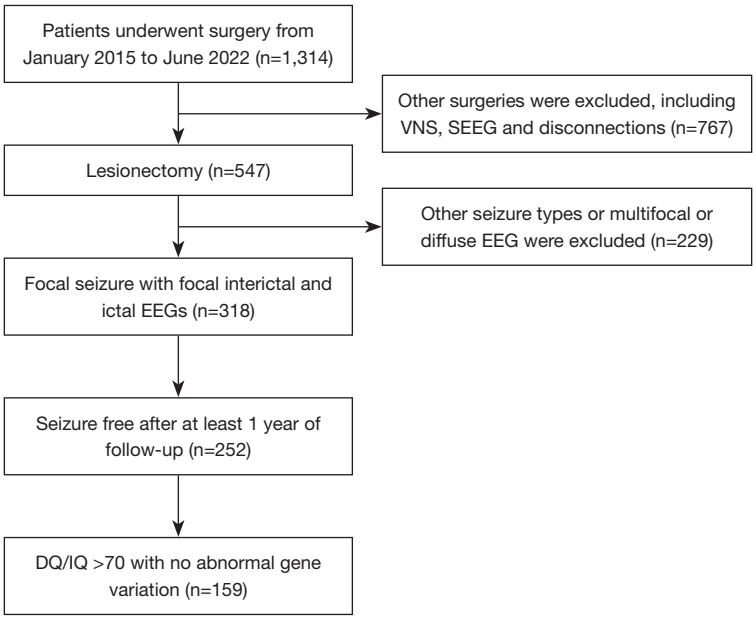

Figure 3 Flowchart of the enrolled patients for modeling. VNS, vagus nerve stimulation; SEEG, stereoelectroencephalography; EEG, electroencephalogram; DQ/IQ, development quotient/intelligence quotient.

Statistical analysis

The voxel-level comparison was implemented through SPM12 software. The detailed statistical methods and parameters are described in the sections above.

Results

Establishment of the PET normal control model

As shown in *Figure 3*, our department performed 1,314 operations on children under the age of 14 years from January 2015 to June 2022. Of these, 547 patients underwent lesionectomy. A total of 318 patients had focal seizures with focal interictal and ictal EEGs. A total of 252 were seizure free, and 93 with DQ/IQ <70 or the presence of genetic variants were excluded. A total of 159 patients (96 boys and 63 girls) who met the requirements were included, including 7 cases in the group of 0~ year olds, 15 cases in the group of 1~ years old, 13 cases in the group of 2~ years old, 15 cases in the group of 3~ years old, 14 cases in the group of 4~ years old, 13 cases in the group of 5~ years old, 14 cases in the group of 6~ years old, 10 cases in the group of 7~ years old, 12 cases in the group of 8~ years old, 9 cases in the group of 9~ years old, 8 cases in the group of 10~ years old, 9 cases in the group of 11~ years old, 10 cases in the group of 12~ years old, and 10 cases in the group of 13~ years old. The epileptogenic zones were located on the left side in 74 cases and on the right side in 85 cases; the epileptogenic zones were located in a single lobe in 133 cases, and in the remaining 26 cases, they were located at the junction of 2 lobes. Patients were seizure free for an average of 2.7 years (1–5 years) of follow-up after surgery.

Model validation

A total of 324 patients meeting the inclusion criteria were screened. In each group, the PET scans of 5 patients were randomly selected for validation. A total of 70 cases (45 boys and 25 girls) with PET data were included in the validation. The epileptogenic zones were located on the left side in 37 cases. In terms of lobe distribution, 32 cases were located in the frontal lobe, 14 cases in the parietal lobe, 23 cases in the temporal lobe, and 1 case in the occipital lobe. In terms of etiology, there were 14 cases of focal cortical dysplasia (FCD) type I, 12 cases of FCD type IIa, 19 cases of FCD type IIb, and 25 cases of long-term epilepsy-associated tumors (LEATs) with or without surrounding FCD. The average ROH was 0.968, with ROH values of 0.939 for FCD I, 0.960 for FCD IIa, 0.980 for FCD IIb, and 0.978 for LEAT. The specific information is detailed in *Table 1*.

Table 1 Information on verified PET

Group	Side (L/R)	Lobe	Pathology	ROH
0~	4/1	Frontal 4, parietal 1	IIa 3, IIb 2	0.985
1~	4/1	Frontal 2, temporal 2, parietal 1	I 1, IIb 2, LEAT 2	0.978
2~	3/2	Frontal 2, temporal 2, parietal 1	IIa 1, IIb 2, LEAT 2	0.985
3~	4/1	Frontal 1, temporal 2, parietal 2	I 2, IIa 1, IIb 1, LEAT 1	0.988
4~	2/3	Frontal 1, temporal 3, parietal 1	I 1, IIa 1, LEAT 3	0.968
5~	3/2	Frontal 1, temporal 2, parietal 2	I 1, IIa 2, IIb 1, LEAT 1	0.963
6~	3/2	Frontal 2, temporal 1, parietal 2	IIb 3, LEAT 2	0.955
7~	3/2	Frontal 3, temporal 2	I 1, IIa 1, IIb 1, LEAT 2	0.964
8~	2/3	Frontal 3, parietal 1, occipital 1	I 1, IIa 1, IIb 1, LEAT 2	0.975
9~	4/1	Frontal 3, temporal 1, parietal 1	I 1, IIb 2, LEAT 2	0.964
10~	0/5	Frontal 2, temporal 3	I 2, IIa 1, LEAT 2	0.956
11~	4/1	Frontal 2, temporal 2, parietal 1	I 2, LEAT 3	0.963
12~	1/4	Frontal 4, temporal 1	IIa 1, IIb 2, LEAT 2	0.932
13~	0/5	Frontal 2, temporal 2, parietal 1	I 2, IIb 2, LEAT 1	0.975

PET, positron emission tomography; L/R, left/right; ROH, ratio of overlapping parts to hypometabolic parts; LEAT, long-term epilepsy-associated tumor.

Analysis of PET changes in children aged 0–14 years

In the 0 to 2~-year-old group, a widespread cortical metabolic increase with greater age was observed, mainly in most of the frontal and occipital cortices. In the 3- to 5~-year-old group, the metabolism of parts of the frontal, parietal, and occipital cortex and caudate nucleus increased with greater age. In the 6- to 9~-year-old group, the areas of increased metabolism were mainly in parts of the frontal lobe, including the supplementary motor area (SMA) and the supramarginal gyrus. In the 10- to 13-year-old group, on the other hand, no significant change in metabolism was observed (*Figure 4*). However, we performed a *t*-test between the 7~- and 13~-year-old groups and found that cortical metabolism was generally higher in the 7~-year-old group than in the 13~-year-old group and was especially pronounced in the posterior head (*Figure 5*).

Discussion

In patients with epilepsy, areas of interictal hypometabolism reflect regions involved in epileptic discharge propagation, whereby the epileptic network can be analyzed by interictal PET (1). It can be inferred that the metabolisms in the areas not involved in epileptic form discharges are likely to be close to those of normal children. Based on the inclusion criteria, we attempted to ensure that children with epileptiform discharges involving only the ipsilateral hemisphere or even 1 ipsilateral brain region were selected. In addition, we selected children with normal genetic testing and a developmental quotient or IQ greater than 70 (18) to ensure that their brain development was essentially normal. All screening criteria were designed to ensure that the contralateral brain was unaffected by abnormal epileptiform discharges and could achieve a metabolic level close to that of normal children. The PET model was then constructed to simulate the data of normal children by the methods described above. The validity was then verified by analyzing the PET of patients who were seizure free after surgery. Patients whose metabolism was defined and roughly overlapped with the surgical resection area were selected. Comparison of the validated PET with the established normal control model revealed that the brain regions with metabolic differences and the surgical resection area were highly overlapping. This confirmed the effectiveness of the normal control model.

The left and right sides of the brain may show different functions and subtle structural and metabolic differences

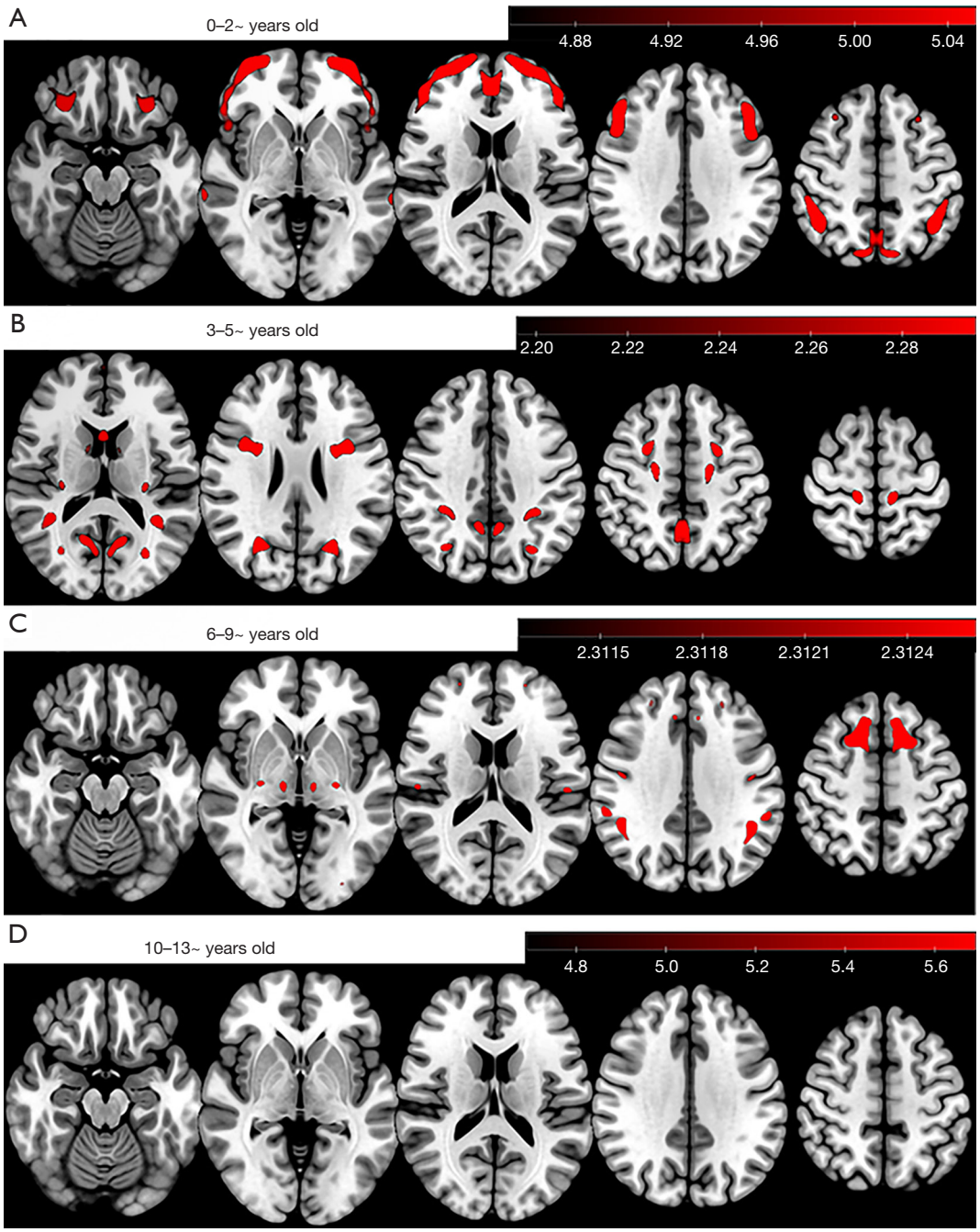

Figure 4 Analysis of the pattern change in patients aged under 14 years. The results of multiple regressions for (A) ages 0–2~ years, (B) 3–5~ years, (C) 6–9~ years, and (D) 10–13~ years are illustrated. (A-C) The age-related increases in metabolism in different brain regions. (D) No significant changes in metabolism.

in adults. Studies have also focused on examining the functional differences between the left and right brain. In the development of the brain in children, although there are some left–right differences, the brain is roughly symmetrical both anatomically and functionally (19). In previous studies of brain networks, flips of the left and right brain have often been used to analyze various networks (3,5). The difference between the left and right sides has a very small effect on

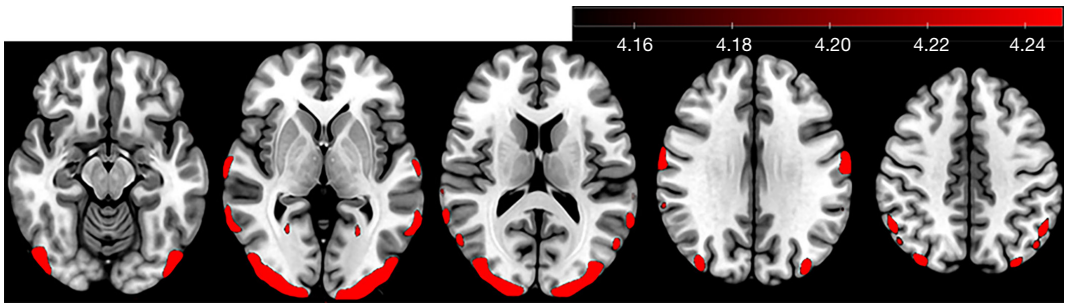

Figure 5 The results of *t*-test between the 7~- and 13~-year-old groups. Cortical metabolism was generally higher in the 7~-year-old group than in the 13~-year-old group and was especially pronounced in the posterior head. The five images showed the axial scans at different levels. The color bar at the top of the graphs indicates the range of the *t* values.

PET analysis. Analysis of PET in normal children and adolescents by Barber *et al.* also suggested that the bilateral brain metabolism is essentially symmetrical during normal development (20). This also demonstrated the feasibility of our methods for establishing the model; however, side remains a factor to be considered in the application of the model.

There are very few studies on brain PET in normal children. One study collected cranial PET data from 28 normal children, but only 5 of them were younger than 6 years old (20). Obtaining normal PET data for young children remains a worldwide challenge, and obtaining PET data for young children that can be grouped by age in a manner adequate for scientific research is even more difficult. In 1987, Chugani *et al.* used PET data from children with transient neurological symptoms to analyze growth and development in children (11). However, during this period, there was a lack of high-resolution imaging equipment. The status of children in the study was determined only by normal CT, and the support of high-resolution MRI to indicate whether there were any intracranial lesions, such as FCD, was lacking. In more recent research, it is more common that PET for those with systemic disease but without intracranial involvement is used to establish a control group (8,21). However, most of the data obtained through this approach have been in older children. Recruitment of healthy people for PET examination, which faces difficulty in being approved by institutional review boards, was reported in a previous study (8). Other studies have used pseudocontrol groups consisting of patients with refractory focal epilepsy but with negative MRI findings and with PET of the hemisphere contralateral to the epileptogenic zone considered normal (22-24). This method is similar to that described in this paper and indicates it was feasible. However, none of these studies have confirmed the reliability of this method, which is one of the implications of this study. This method may provide convenience to future studies in analyzing brain epileptic networks in children, lesion detection, SEEG planning, postoperative identification of residual lesions, etc.

Based on our normal model data, multiple regression analyses were performed for each 3- to 4-year age interval and suggested that significant changes were found in brain metabolism according to age. The cerebral metabolic changes with age in children within the first 6 years essentially involved most of the cerebral cortex. Especially at 0–3 years of age, there was a significant age-related metabolic increase in the majority of the frontal and occipital cortices. Since glucose and oxygen are fundamental to meeting the energy demands of the brain, many PET studies of early development have measured age changes and differences in these substrates (25-27). Increased metabolism over the range of 0–6 years of age may be associated with changes in the volume of the cerebral cortex and the formation and refinement of functions in the corresponding brain regions (28,29). At this time, brain development is active and has a substantial influence on metabolism. By 6 years of age, the brain volume approaches 95% of that of adults, and after 6 years of age, the number of brain regions with metabolic changes decreases, with metabolism reaching a plateau (11,30).

Chugani *et al.* concluded that brain metabolism reaches its peak between the ages of 8 and 10 years, with a gradual decline in metabolic levels after 10 years of age (11). In our study, we found a gradual increase in metabolism in different brain regions from 0–10 years of age. However, our multiple regression analysis for the 10- to 13~-year-old

group did not reveal age-related metabolic increases or decreases. However, we compared the PET scans between the 7~- and 13~-year-old groups and found that posterior head metabolism was significantly higher in the 7~-year-old group. This corroborates some of the findings of Chugani *et al.* that there may be a slow decline in metabolism after 10 years of age, but this trend may be nonlinear. By age 14 years, metabolic levels are essentially close to those of adults (31). Therefore, in network analyses, it is inappropriate to use adult normal control data to analyze children's PET scan, especially for children aged 0–6 years. This also indicates that our modeling is necessary.

The metabolism of several brain lobes increases with age up to the age of 10 years, reflecting synaptic proliferation (32) and the emergence of corresponding function (11). During childhood development, motor, language, and visual functions gradually mature, and these functions are widely distributed in the frontal, parietal, and occipital cortices. The accelerating loss of gray-matter density may explain the metabolism decrease at the ages from 10 to 17 years (9).

The next step of research is to increase the number of cases in each group, especially in the group of younger children. When the sample size is sufficiently large, we can consider creating a database using these PET data. We are also contemplating embedding the database into the software to facilitate subsequent quantitative analysis of PET.

Limitations

Some limitations of our study should be mentioned. First, it is difficult to obtain data for children aged 0–1 years. As most of the epilepsy patients aged 0–1 years had large lesions, the data that met our modeling requirements were highly scarce. In the end, there were only 7 cases with data that met the requirements. We will continue to add to this group in the coming years as the number of patients increases. Second, the model we established can only approximate normal children and cannot completely replace them. Third, a previous study reported a slight reduction in the cerebral metabolic rates of glucose in brain regions, but cerebral blood flow (CBF) was unaltered via chloral intake (33). The majority of patients in the group aged 0–3 years required sedation. For regression analyses, patients aged 0–3 years were grouped together for analysis, and biases might have arisen due to sedation. However, maintaining stillness during the examination is crucial in pediatric imaging, as minor movements can lead to artifacts (34), thus necessitating sedation in younger children.

Conclusions

This study is the first to demonstrate the feasibility of mirroring the contralateral hemisphere of the epileptic zone and splicing it into a complete brain in establishing a normal control group. The prerequisite for this method is that the data used for modeling should be strictly screened to avoid discharge involvement of the contralateral hemisphere. Children under 10 years old, especially within 3 years of age, show pronounced changes in brain metabolism with each additional year of age, and metabolism decreases nonlinearly after 10 years of age.

Acknowledgments

Funding: We are grateful for funding from the National Natural Science Foundation of China (No. 82201601 to Y.W.) and CAAE Epilepsy Research Funding (No. CU-2022-036 to Y.W.).

Footnote

Reporting Checklist: The authors have completed the STROBE reporting checklist. Available at https://qims.amegroups.com/article/view/10.21037/qims-23-1809/rc

Conflicts of Interest: All authors have completed the ICMJE uniform disclosure form (available at https://qims.amegroups.com/article/view/10.21037/qims-23-1809/coif). Y.W. reports support funding from the National Natural Science Foundation of China (No. 82201601) and CAAE Epilepsy Research Funding (No. CU-2022-036). The other authors have no conflicts of interest to declare.

Ethical Statement: The authors are accountable for all aspects of the work in ensuring that questions related to the accuracy or integrity of any part of the work are appropriately investigated and resolved. This study was conducted in accordance with the Declaration of Helsinki (as revised in 2013) and was approved by the Institutional Review Board of Peking University First Hospital (protocol code: 2022-306-001; date: July 7, 2022). Informed consent was obtained from the patients' parents or legal guardians.

References

1. Chassoux F, Semah F, Bouilleret V, Landre E, Devaux B, Turak B, Nataf F, Roux FX. Metabolic changes and electro-clinical patterns in mesio-temporal lobe epilepsy: a correlative study. Brain 2004;127:164-74.
2. Obaid S, Tucholka A, Ghaziri J, Jodoin PM, Morency F, Descoteaux M, Bouthillier A, Nguyen DK. Cortical thickness analysis in operculo-insular epilepsy. Neuroimage Clin 2018;19:727-33.
3. Wang Y, Wang X, Mo JJ, Sang L, Zhao BT, Zhang C, Hu WH, Zhang JG, Shao XQ, Zhang K. Symptomatogenic zone and network of oroalimentary automatisms in mesial temporal lobe epilepsy. Epilepsia 2019;60:1150-9.
4. Soncin LD, Faure S, McGonigal A, Horowitz T, Belquaid S, Bartolomei F, Guedj E. Correlation between fluorodeoxyglucose positron emission tomography brain hypometabolism and posttraumatic stress disorder symptoms in temporal lobe epilepsy. Epilepsia 2022;63:e74-9.
5. Zhang C, Zhao BT, McGonigal A, Hu WH, Wang X, Shao XQ, Ma YS, Zhang JG, Zhang K. Superior Frontal Sulcus Focal Cortical Dysplasia Type II: An MRI, PET, and Quantified SEEG Study. Front Neurol 2019;10:1253.
6. Sinha N, Wang Y, Moreira da Silva N, Miserocchi A, McEvoy AW, de Tisi J, Vos SB, Winston GP, Duncan JS, Taylor PN. Structural Brain Network Abnormalities and the Probability of Seizure Recurrence After Epilepsy Surgery. Neurology 2021;96:e758-71.
7. Vaughan DN, Rayner G, Tailby C, Jackson GD. MRI-negative temporal lobe epilepsy: A network disorder of neocortical connectivity. Neurology 2016;87:1934-42.
8. Li Y, Zhang T, Feng J, Qian S, Wu S, Zhou R, Wang J, Sa G, Wang X, Li L, Chen F, Yang H, Zhang H, Tian M. Processing speed dysfunction is associated with functional corticostriatal circuit alterations in childhood epilepsy with centrotemporal spikes: a PET and fMRI study. Eur J Nucl Med Mol Imaging 2022;49:3186-96.
9. Cruz-Cortes Á, Avendaño-Estrada A, Alcauter S, Núñez-Enríquez JC, Rivera-Bravo B, Olarte-Casas MÁ, Ávila-Rodríguez MÁ. Semiquantitative analysis of cerebral [18F] FDG-PET uptake in pediatric patients. Pediatr Radiol 2023;53:2574-85.
10. Wang H, Tian Y, Liu Y, Chen Z, Zhai H, Zhuang M, Zhang N, Jiang Y, Gao Y, Feng H, Zhang Y. Population-specific brain [18F]-FDG PET templates of Chinese subjects for statistical parametric mapping. Sci Data 2021;8:305.
11. Chugani HT, Phelps ME, Mazziotta JC. Positron emission tomography study of human brain functional development. Ann Neurol 1987;22:487-97.
12. Stadskleiv K. Cognitive functioning in children with cerebral palsy. Dev Med Child Neurol 2020;62:283-9.
13. Stefanos-Yakoub I, Wingeier K, Held U, Latal B, Wirrell E, Smith ML, Ramantani G. Long-term intellectual and developmental outcomes after pediatric epilepsy surgery: A systematic review and meta-analysis. Epilepsia 2024;65:251-65.
14. Fonov V, Evans AC, Botteron K, Almli CR, McKinstry RC, Collins DL; Brain Development Cooperative Group. Unbiased average age-appropriate atlases for pediatric studies. Neuroimage 2011;54:313-27.
15. Fonov VS, Evans AC, McKinstry RC, Almli CR, Collins DL. Unbiased nonlinear average age-appropriate brain templates from birth to adulthood. NeuroImage 2009;47:S102.
16. von Below D, Wallerstedt SM, Bergquist F. Validation of the Swedish Patient-Reported Outcomes in Parkinson's Disease Scale in Outpatients. Mov Disord 2023;38:1668-78.
17. Mo J, Dong W, Cui T, Chen C, Shi W, Hu W, Zhang C, Wang X, Zhang K, Shao X. Whole-brain metabolic pattern analysis in patients with anti-leucine-rich glioma-inactivated 1 (LGI1) encephalitis. Eur J Neurol 2022;29:2376-85.
18. Morningstar M, Hung A, Mattson WI, Gedela S, Ostendorf AP, Nelson EE. Internalizing symptoms in intractable pediatric epilepsy: Structural and functional brain correlates. Epilepsy Behav 2020;103:106845.
19. Duboc V, Dufourcq P, Blader P, Roussigné M. Asymmetry of the Brain: Development and Implications. Annu Rev Genet 2015;49:647-72.
20. Barber TW, Veysey D, Billah B, Francis P. Normal brain metabolism on FDG PET/MRI during childhood and adolescence. Nucl Med Commun 2018;39:1022-32.
21. Zhang Q, Liao Y, Wang X, Zhang T, Feng J, Deng J, et al. A deep learning framework for 18F-FDG PET imaging diagnosis in pediatric patients with temporal lobe epilepsy.

Eur J Nucl Med Mol Imaging 2021;48:2476-85.
22. Balfroid T, Warren AEL, Dalic LJ, Aeby A, Berlangieri SU, Archer JS. Frontoparietal (18)F-FDG-PET hypometabolism in Lennox-Gastaut syndrome: Further evidence highlighting the key network. Epilepsy Res 2023;192:107131.
23. Archambaud F, Bouilleret V, Hertz-Pannier L, Chaumet-Riffaud P, Rodrigo S, Dulac O, Chassoux F, Chiron C. Optimizing statistical parametric mapping analysis of 18F-FDG PET in children. EJNMMI Res 2013;3:2.
24. Macdonald-Laurs E, Warren AEL, Lee WS, Yang JY, MacGregor D, Lockhart PJ, Leventer RJ, Neal A, Harvey AS. Intrinsic and secondary epileptogenicity in focal cortical dysplasia type II. Epilepsia 2023;64:348-63.
25. Chugani HT, Phelps ME. Imaging human brain development with positron emission tomography. J Nucl Med 1991;32:23-6.
26. Muzik O, Janisse J, Ager J, Shen C, Chugani DC, Chugani HT. A mathematical model for the analysis of cross-sectional brain glucose metabolism data in children. Prog Neuropsychopharmacol Biol Psychiatry 1999;23:589-600.
27. Takahashi T, Shirane R, Sato S, Yoshimoto T. Developmental changes of cerebral blood flow and oxygen metabolism in children. AJNR Am J Neuroradiol 1999;20:917-22.
28. Sowell ER, Thompson PM, Leonard CM, Welcome SE, Kan E, Toga AW. Longitudinal mapping of cortical thickness and brain growth in normal children. J Neurosci 2004;24:8223-31.
29. Zhong J, Rifkin-Graboi A, Ta AT, Yap KL, Chuang KH, Meaney MJ, Qiu A. Functional networks in parallel with cortical development associate with executive functions in children. Cereb Cortex 2014;24:1937-47.
30. Lenroot RK, Giedd JN. Brain development in children and adolescents: insights from anatomical magnetic resonance imaging. Neurosci Biobehav Rev 2006;30:718-29.
31. Grant FD. Normal variations and benign findings in pediatric 18F-FDG-PET/CT. PET Clin 2014;9:195-208.
32. Changeux JP, Danchin A. Selective stabilisation of developing synapses as a mechanism for the specification of neuronal networks. Nature 1976;264:705-12.
33. Suzuki C, Kosugi M, Magata Y. Conscious rat PET imaging with soft immobilization for quantitation of brain functions: comprehensive assessment of anesthesia effects on cerebral blood flow and metabolism. EJNMMI Res 2021;11:46.
34. Zhou X, Fu Y, Dong S, Li L, Xue S, Chen R, Huang G, Liu J, Shi K. Intelligent ultrafast total-body PET for sedation-free pediatric [18F]FDG imaging. Eur J Nucl Med Mol Imaging 2024;51:2353-66.

Cite this article as: Wang Y, Mo J, Sun Y, Yu H, Liu C, Liu Q, Fan Y, Wang S, Liu X, Jiang Y, Cai L. Establishment of a normal control model of children's brain 18-fluorodeoxyglucose positron emission tomography and analysis of the changing pattern in patients aged 0–14 years. Quant Imaging Med Surg 2024;14(7):4703-4713. doi: 10.21037/qims-23-1809

